

Optical properties of a nonlinear magnetic charged rotating black hole surrounded by quintessence with a cosmological constant

Yuan Chen, He-Xu Zhang, Tian-Chi Ma, and Jian-Bo Deng*

Institute of Theoretical Physics & Research Center of Gravitation,

Lanzhou University, Lanzhou 730000, China

(Dated: April 28, 2021)

Abstract

In this paper, we discuss optical properties of the nonlinear magnetic charged black hole surrounded by quintessence with a non-zero cosmological constant Λ . Setting the state parameter $\omega = -3/2$, we studied the horizon, the photon region and the shadow of this black hole. It turned out that for a fixed quintessential parameter γ , in a certain range, with the increase of the rotation parameter a and magnetic charge Q , the inner horizon radius increases while the outer horizon radius decreases. And the cosmological horizon r_Λ decrease when γ or Λ increase and increase slightly with increasing a and Q . The shapes of photon region were then studied and depicted through graphical illustrations. Finally, we discussed the effects of the quintessential parameter γ and the cosmological constant Λ on the shadow cast by this black hole with a fixed observer position.

* Jian-Bo Deng: dengjb@lzu.edu.cn

I. INTRODUCTION

Modern cosmological observations reveal that most galaxies may contain supermassive black holes in their centers. As an instance, astrophysical observations expect that there is a black hole lying at the center of our galaxy. Recently, a project, named the Event Horizon Telescope[1], is successfully collecting signals from radio sources. And it may help us testing the theory of general relativity in the strong-field regime. So it is necessary to study the optical properties theoretically, so that we can provide a reference substance for future observation.

The photon sphere is a spherical surface round a black hole without rotation, which containing all the possible closed orbits of a photon. But for a black hole with rotation, there is no longer a sphere but a region which is broken from the photon sphere. It is a region which is filled by spherical lightlike geodesics. The light rays that asymptotically spiral towards one of these spherical lightlike geodesics corresponds to boundary of the shadow. So the property of photon region takes great significance to the research of black hole shadow, which is an important project in black hole observation.

The shadow of a black hole is a natural consequence from the general theory of gravity. And even there is many the different methods employed to determine the nature of the black hole, observation of the shadow of a black hole remains probably the most interesting one. The shadow of a spherically symmetric black hole appear as a perfect circle, which was first studied by Synge[2]. And then the spherically symmetric black hole with an accretion disk was discussed by Luminet[3]. The shapes of shadows of black holes with rotation take deformation, and Bardeen was the first one to correctly calculate it[4]. Recent astrophysical observation have motivated many authors to study of shadows in theoretical investigation, like Kerr-Newman black holes[5], naked singularities with deformation parameters[6], multi-

black holes[7] and Kerr-NUT spacetimes [8]. And some authors tried to test theories of gravity by using the observations of shadow obtained from the black hole lying in our galaxy[9–11].

In present view, the cosmological constant has been considered to have the potential to explain several theoretical and observational problems, for example, as a possible cause of the observed acceleration of the universe. And one of the strongest supports was the results of the observation for a supernova[12], which suggests the probable presence of a positive cosmological constant for our universe. Therefore studying black holes with a non-zero cosmological constant has an significant place in research. Many authors studied black holes with a non-zero cosmological constants[13–17] And it should be noted that in the case with a non-zero cosmological constant the traditional method to compute shadow, which place observers at near infinite distance, is no longer valid. So we will take a different method, following[18].

Recent cosmological observations suggest that our current universe contains mainly of 68.3% dark energy , 26.8% dark matter, and 4.9% baryon matter, according to the Standard Model of Cosmology [19]. Thus, it is necessary to consider dark matter or dark energy in the black hole solutions. In recent years, the black hole surrounded by quintessence dark energy have caught a lot of attention. For example, Kiselev [20] considered the Schwarzschild black hole surrounded by the quintessential energy and then Toshmatov and Stuchlík [21] extended it to the Kerr-like black hole; the quasinormal modes, thermodynamics and phase transition from Bardeen Black hole surrounded by quintessence was discussed by Saleh and Thomas [22]; the Hayward black holes surrounded by quintessence have been studied in Ref. [23], etc [24–29], see Refs. [30–37] for more recent research. And some authors have considered black holes surrounded by quintessence with a non-zero cosmological constant[38–42]. And for discussing the effects of cosmological background of black holes, we will consider quintessence in our work.

Our paper is organized as follows. In the next section, we give the solution of nonlinear magnetic charged rotating black hole surrounded by quintessence including a cosmological constant. The horizons is the subject of Sec. III. In Sec. IV, we study the photon region. And the shadows are discussed in Sec. V. Conclusions and discussions are presented in Sec. VI. For simplicity, the quintessential state parameter ω and mass M will be set to $-2/3$ and 1 , respectively.

II. THE METRIC OF NONLINEAR MAGNETIC CHARGED ROTATING BLACK HOLE SURROUNDED BY QUINTESSENCE WITH A COSMOLOGICAL CONSTANT

Kiselev first derived the solutions of the black hole surrounded by the quintessence [20]. Then, it have been applied in many articles. As a result of applying, the solution of nonlinear magnetic-charged black hole surrounded by quintessence was obtained in Ref.[43] by considering Einstein gravity coupled to a nonlinear electromagnetic field. And recently the solution has been generalized to include rotation[23]. And the rotational version is given by

$$ds^2 = -\frac{\Delta_r}{\Sigma} (dt - a \sin^2 \theta d\phi)^2 + \frac{\Sigma}{\Delta_r} dr^2 + \Sigma d\theta^2 + \frac{\sin^2 \theta}{\Sigma} (adt - (r^2 + a^2) d\phi)^2 \quad (1)$$

with

$$\Sigma = r^2 + a^2 \cos^2 \theta, \Delta_r = r^2 + a^2 - \frac{2Mr^4}{r^3 + Q^3} - \gamma r^{1-3\omega}. \quad (2)$$

where the a is a rotational parameter, Q is magnetic charge, ω is a state parameter and γ is the quintessential parameter.

Considering Einstein equation with a positive cosmological constant, it takes the form

$$\tilde{G}_{\mu\nu} = R_{\mu\nu} - \frac{1}{2}Rg_{\mu\nu} + \Lambda g_{\mu\nu} = 8\pi T_{\mu\nu}. \quad (3)$$

With the cosmological constant, we assume the solution including a cosmological constant is

$$ds^2 = -\frac{\Delta_r}{\Xi^2 \Sigma} (dt - a \sin^2 \theta d\phi)^2 + \frac{\Sigma}{\Delta_r} dr^2 + \frac{\Sigma}{\Delta_\theta} d\theta^2 + \frac{\Delta_\theta \sin^2 \theta}{\Xi^2 \Sigma} (adt - (r^2 + a^2) d\phi)^2, \quad (4)$$

with

$$\begin{aligned} \Xi &= 1 + \frac{\Lambda}{3} a^2, \Sigma = r^2 + a^2 \cos^2 \theta, \Delta_\theta = 1 + \frac{\Lambda}{3} a^2 \cos^2 \theta, \\ \Delta_r &= r^2 + a^2 - \frac{2Mr^4}{r^3 + Q^3} - \gamma r^{1-3\omega} - \frac{\Lambda}{3} (r^2 + a^2) r^2. \end{aligned} \quad (5)$$

With the help of Mathematica, we find the metric (4) actually satisfies Einstein equation (3) coupling with a non-linear electromagnetic field in quintessence with a cosmological constant. The solution reduce to nonlinear magnetic charged solution when $\Lambda = 0$, $a = 0$, and $\gamma = 0$. And when $\Lambda = 0$, $a = 0$, $Q = 0$ and $\gamma = 0$, it come back to Schwarzschild spacetime.

III. HORIZON

Similar to the Kerr black hole, the space-time metric (4) is singular at $\Delta_r = 0$, which corresponds to the horizons of the rotating black hole. In other words, the horizons are solutions of

$$\Delta_r = r^2 + a^2 - \frac{2Mr^4}{r^3 + Q^3} - \gamma r^3 - \frac{\Lambda}{3} (r^2 + a^2) r^2 = 0. \quad (6)$$

Obviously, the radii of horizons depend on the rotation parameter a , magnetic charge Q , quintessence parameter γ and the cosmological constant Λ . This equation is unable to solved analytically. When Λ is positive, the numerical analysis of Eq. (6) suggests the possibility of three roots for a set of values of parameters, which correspond the inner horizon r_- (smaller root), the outer horizon r_+ (larger root) and the cosmological horizon r_Λ (the largest root), respectively. The variation of Δ_r

with respect to r for the different values of parameters a , with fixed Q , γ and Λ is depicted in Figs. 1 and the roots of $\Delta_r = 0$ with varying a has been listed in Tab. I and Tab II. As can be seen from Fig. 1, Tab. I and Tab II, for fixed parameters Q , γ and Λ , if $a < a_E$, the radii of outer horizons decrease with the increasing a while the radii of inner horizons increase. For $a = a_E$, r_- and r_+ meet at r_E , i.e. we have an extreme case which inner horizons and outer horizons degenerate. The critical rotation parameter a_E and the corresponding critical radius r_E can be calculated by combining $\Delta_r = 0$ with $\frac{d\Delta_r}{dr} = 0$. When $a > a_E$, inner horizon and outer horizon will not exist any more, which means there is no longer a black hole. At the same time, r_Λ increase as a increase but not so obviously.

A similar analysis can be applied to Q . We list the roots in Tab.III with varying Q in the case $a = 0.2$, $\gamma = 0.01$ and $\Lambda = 0.02$ and depict the variation of Δ_r with respect to r for the different values of parameters Q with fixed a , γ and Λ in Fig. 2. The result shows that, for any given values of parameters a , γ and Λ , inner and outer horizons get closer first with the increase of Q , then coincide when $Q = Q_E$ and disappear when $Q > Q_E$. And r_Λ increase as Q increase but not so significantly.

Then, we further analyze the behavior of the horizons under different values of quintessence parameter and cosmological constant. For simplicity, we set $Q = 0.2$ and consider the different values of cosmological constant Λ and quintessential parameter γ , then vary the value of a in the interval $0 < a < 1$, find the roots and list them in Tab I and Tab I. From the Tables, we can see that with fixed a the cosmological horizon r_Λ significantly decrease while r_+ increase as γ or Λ increase.

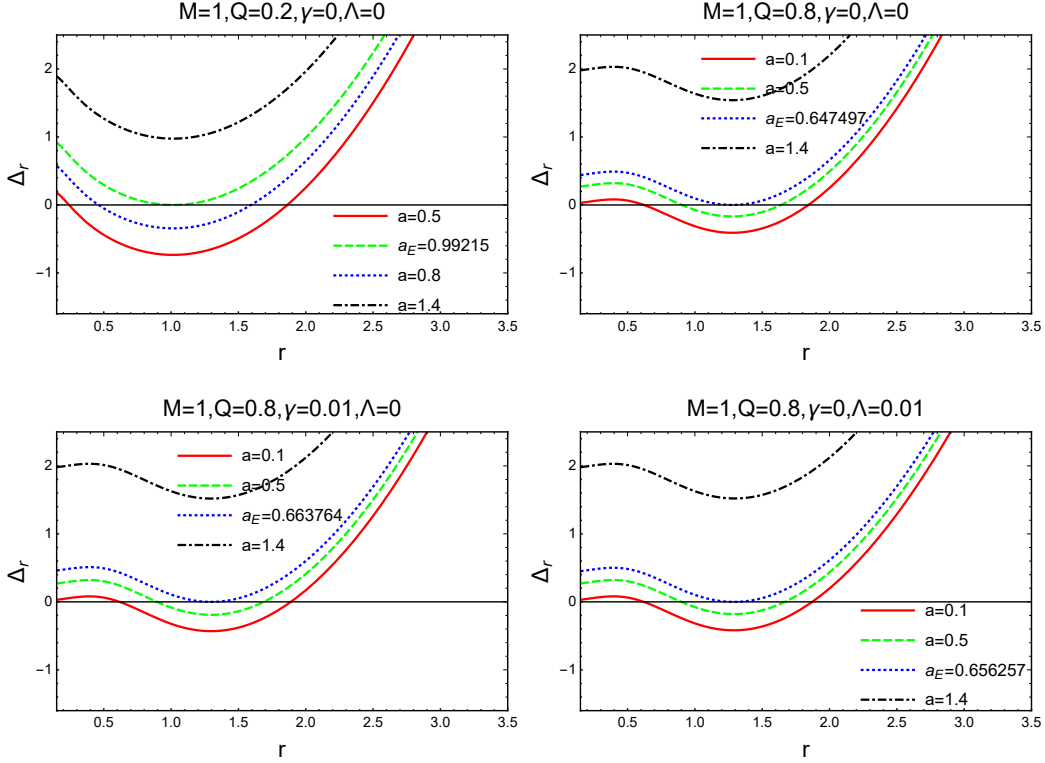


Figure 1: Plot showing the behavior of horizons vs r for a set of fixed values of Q , γ and Λ by varying a .

IV. PHOTON REGION

In this section, we turn to the property of the photon region. For the spacetime (4), geodesic motion can be governed by the Hamilton Jacobi equation [22],

$$\frac{\partial S}{\partial \tau} = -\frac{1}{2}g^{\mu\nu} \frac{\partial S}{\partial x^\mu} \frac{\partial S}{\partial x^\nu}. \quad (7)$$

where the τ is the affine parameter, x^μ represents the 4-vector, and S is the Hamilton-Jacobi action function for a test particle, which can be written in following form:

$$S = \frac{1}{2}m^2\tau - Et + L\phi + S_r(r) + S_\theta(\theta). \quad (8)$$

Then, by inserting the metric tensor of spacetime (4) and Eq. (8) to Eq. (7), we obtain

$$m^2 = \frac{\Xi^2((r^2 + a^2)^2 \Delta_\theta - a^2 \sin^2(\theta) \Delta_r)}{\Delta_\theta \Delta_r \Sigma} E^2 - \frac{\Delta_r}{\Sigma} \left(\frac{\partial S_r(r)}{\partial r} \right)^2 - \frac{\Delta_\theta}{\Sigma} \left(\frac{\partial S_\theta(\theta)}{\partial \theta} \right)^2 - \frac{\Xi^2(-a^2 \Delta_\theta + \csc^2(\theta) \Delta_r)}{\Delta_\theta \Delta_r \Sigma} L^2 - \frac{2a\Xi^2((r^2 + a^2) \Delta_\theta - \Delta_r)}{\Delta_\theta \Delta_r \Sigma} EL. \quad (9)$$

By using the separation of variables method and introducing the Carter constant

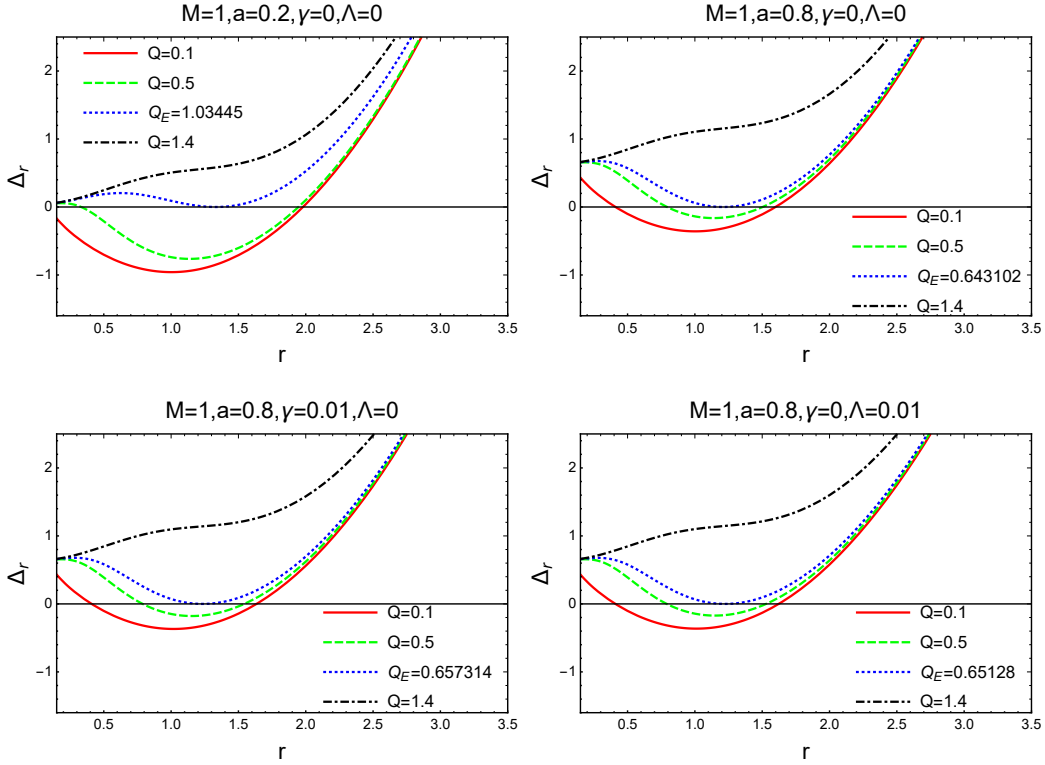


Figure 2: Plot showing the behavior of horizons vs r for a set of fixed values of a , γ and Λ by varying Q .

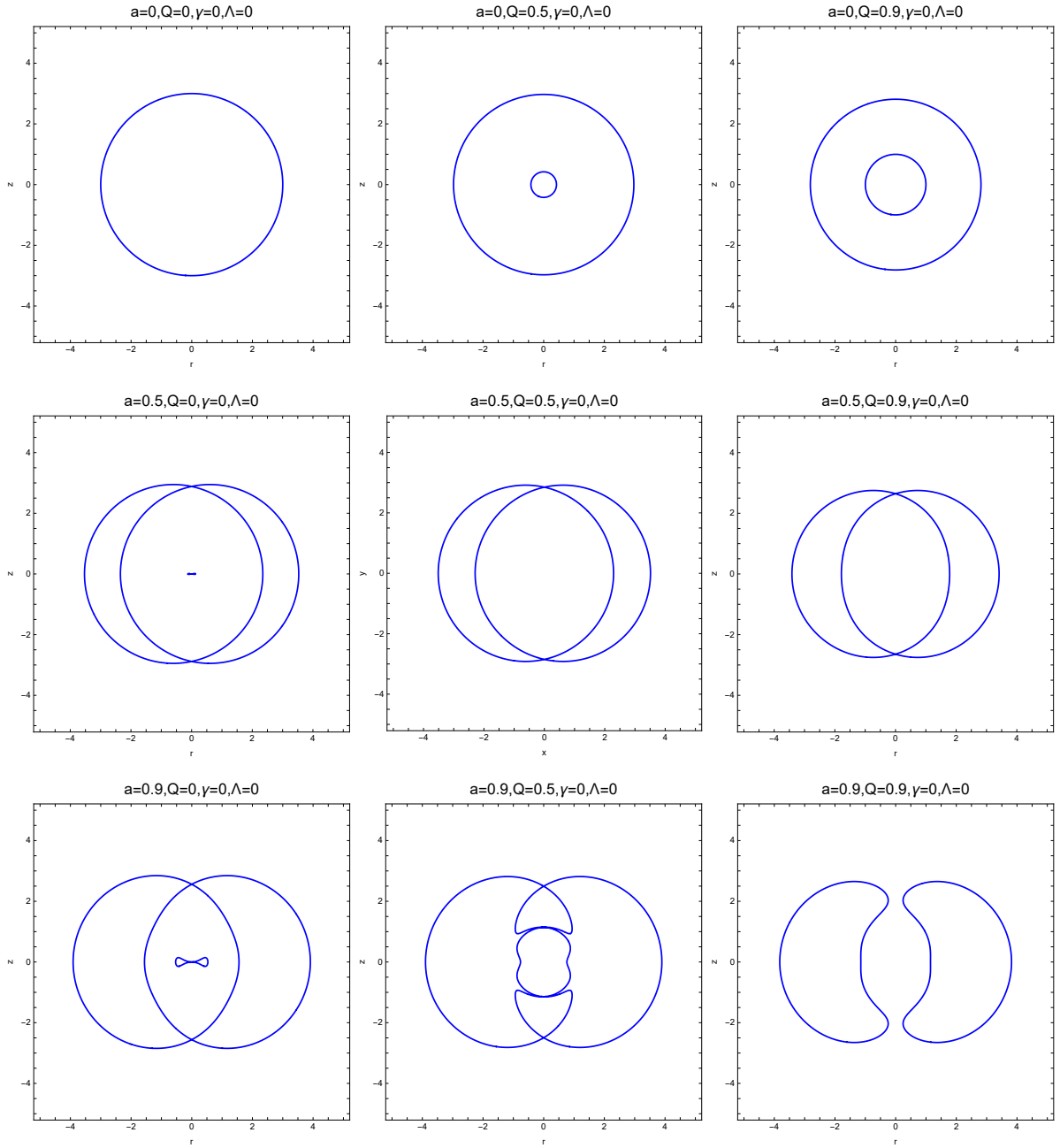


Figure 3: Shape of photon regions with $\Lambda = 0$ and $\gamma = 0$ for a set of values of parameters Q and a .

Table I: The radii of horizons for a set of fixed values of $Q = 0.2$ and $\Lambda = 0.01$ by varying a in different values of γ

a	$\gamma = 0.01$			$\gamma = 0.02$			$\gamma = 0.03$		
	r_-	r_+	r_Λ	r_-	r_+	r_Λ	r_-	r_+	r_Λ
0	0.06427	2.071	14.666	0.06424	2.120	13.2381	0.06422	2.175	11.930
0.1	0.09616	2.065	14.6661	0.09614	2.114	13.2384	0.09613	2.169	11.9308
0.2	0.13072	2.050	14.6665	0.13069	2.098	13.2391	0.13068	2.152	11.932
0.3	0.16415	2.023	14.6672	0.16413	2.071	13.2403	0.16410	2.124	11.9339
0.4	0.19995	1.984	14.6681	0.1999	2.031	13.242	0.19987	2.083	11.9366
0.5	0.24154	1.931	14.6693	0.24147	1.977	13.2442	0.24141	2.028	11.9401
0.6	0.29343	1.863	14.6708	0.29331	1.907	13.2469	0.29318	1.956	11.9443
0.7	0.36245	1.774	14.6725	0.36217	1.817	13.2501	0.36190	1.863	11.9492
0.8	0.45992	1.656	14.6745	0.45921	1.697	13.2537	0.45851	1.742	11.9549

Table II: The radii of horizons for a set of fixed values of $Q = 0.2$ and $\gamma = 0.01$ by varying a in different values of Λ .

a	$\Lambda = 0.01$			$\Lambda = 0.02$			$\Lambda = 0.03$		
	r_-	r_+	r_Λ	r_-	r_+	r_Λ	r_-	r_+	r_Λ
0	0.06427	2.071	14.666	0.06426	2.105	10.2654	0.06426	2.143	8.2118
0.1	0.09616	2.065	14.6661	0.09616	2.099	10.2656	0.09616	2.137	8.2121
0.2	0.13072	2.050	14.6665	0.13072	2.083	10.2662	0.13071	2.121	8.2131
0.3	0.16415	2.023	14.6672	0.16414	2.056	10.2673	0.16414	2.093	8.2148
0.4	0.19995	1.984	14.6681	0.19993	2.016	10.2689	0.19992	2.052	8.2171
0.5	0.24154	1.931	14.6693	0.24151	1.963	10.2709	0.24148	1.997	8.2201
0.6	0.29343	1.863	14.6708	0.29337	1.893	10.2733	0.29330	1.926	8.2237
0.7	0.36245	1.774	14.6725	0.36229	1.803	10.2761	0.36213	1.835	8.2279
0.8	0.45992	1.656	14.6745	0.45948	1.684	10.2793	0.45905	1.714	8.2328

Table III: The radii of horizons for a set of fixed values of $a = 0.2$ and $\gamma = 0.01, \Lambda = 0.01$ by varying Q .

Q	$\Lambda = 0.01, \gamma = 0.01$		
	r_-	r_+	r_Λ
0	0.02020	2.0853	10.2662
0.1	0.07565	2.0851	10.2662
0.2	0.11461	2.0832	10.2662
0.3	0.13071	2.0783	10.2663
0.4	0.18902	2.0687	10.2663
0.5	0.25485	2.0523	10.2664
0.6	0.33126	2.0268	10.2665
0.7	0.42101	1.9889	10.2667
0.8	0.65584	1.9329	10.267

K , we can arrive at

$$\frac{dS_r(r)}{dr} = \frac{\sqrt{R(r)}}{\Delta_r}, \quad (10)$$

$$\frac{dS_\theta(\theta)}{d\theta} = \frac{\sqrt{\Theta(\theta)}}{\Delta_\theta}, \quad (11)$$

where

$$R(r) = (aL - (a^2 + r^2)E)^2 \Xi^2 - m^2 r^2 \Delta_r - K \Delta_r, \quad (12)$$

$$\Theta(\theta) = K \Delta_\theta - a^2 m^2 \cos^2(\theta) - \Xi^2 (L \csc(\theta) - aE \sin(\theta))^2. \quad (13)$$

With these forms, we can rewrite the Hamilton-Jacobi function as

$$S = \frac{1}{2} m^2 \tau - Et + L\phi + \int^r \frac{\sqrt{R(r)}}{\Delta_r} dr + \int^\theta \frac{\sqrt{\Theta(\theta)}}{\Delta_\theta} d\theta. \quad (14)$$

Following [?], we write geodesic motion in the form

$$\Sigma \frac{dt}{d\tau} = \frac{\Xi^2((r^2 + a^2)E - aL)(r^2 + a^2)}{\Delta_r} - \frac{a\Xi^2(aE \sin^2(\theta) - L)}{\Delta_\theta}, \quad (15)$$

$$\Sigma \frac{dr}{d\tau} = \sqrt{R(r)}, \quad (16)$$

$$\Sigma \frac{d\theta}{d\tau} = \sqrt{\Theta(\theta)}, \quad (17)$$

$$\Sigma \frac{d\phi}{d\tau} = \frac{a\Xi^2((r^2 + a^2)E - aL)}{\Delta_r} - \frac{\Xi^2(aE \sin^2(\theta) - L)}{\Delta_\theta \sin^2(\theta)}. \quad (18)$$

Here, we're interested in lightlike geodesics that stay on a sphere with a constant radius. For lightlike geodesics, m of test particle is zero. The region filled by these geodesics can be called as the photon region.

The conditions $\frac{dr}{d\tau} = 0$ and $\frac{d^2r}{d\tau^2} = 0$ must be satisfied simultaneously to get spherical orbits, which means that

$$R(r) = 0, \quad \frac{dR(r)}{dr} = 0. \quad (19)$$

For simplicity, we introduce two reduced parameters $\xi = \frac{L}{E}, \eta = \frac{K}{E^2}$. By solving above equations, we can obtain ξ and η for limiting spherical lightlike geodesic, by

$$a\xi = r_p^2 + a^2 - 4\frac{r\Delta_r}{\Delta'_r}, \quad (20)$$

$$\eta = \frac{16r^2\Xi^2\Delta_r}{(\Delta'_r)^2}. \quad (21)$$

Inserting (20) and (21) into $\Theta \geq 0$, we find the condition which describes the photon region. We will discuss th photon regions in (r, θ) plane

$$16r^2a^2\Delta_r\Delta_\theta \sin^2(\theta) - (4r\Delta_r - \Sigma\Delta'_r)^2 \geq 0. \quad (22)$$

And we have shown the shape of photon region with different values of a, Q, γ and Λ in Fig. 3 and Fig. 4. From the picture, we can see some interesting phenomenon.

For example, when $a = 0$, Eq. (22) reduces to

$$(4r\Delta_r - \Sigma\Delta'_r)^2 = 0. \quad (23)$$

And it means that photon regions reduce to photon spheres. In Schwarzschild

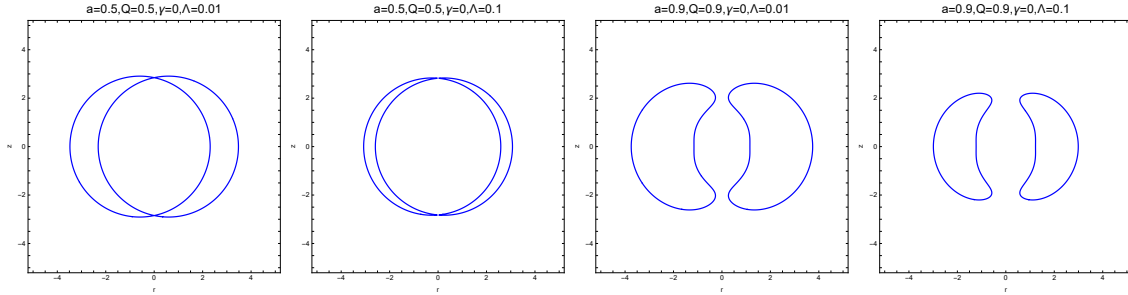


Figure 4: Shape of photon regions with fixed a and Q for a set of values of parameters Λ

space-time, i.e , a , Q , γ and Λ become zero simultaneously, the photon sphere stay at $r = 3$. When $a = 0$ with a non-zero Q , there will be two photon spheres. And the radiu of inner photon sphere increase as Q increases. With increasing a , the photon sphere will expand to two crescent-shaped axisymmetric region in (r, θ) plane and a interior photon region will rise. And non-zero Q will diminish the area enclosed by the two crescent-shaped photon region. Keeping increasing Q , the exterior photon regions will touch the interior photon region, get deformation with the disappearance of interior regions. For a large Q , photon regions will separate into two untouched regions. From Fig. 4, we can see that photon regions will shrink with a increasing Λ . For quintessential parameter γ , it gets more interesting, as there can be two different situation.

Type I. For a small a and Q , two exterior photon regions maintain crescent shape and keep touching each other. Increasing value of γ will stretch the photon regions to both sides and diminish the regions. See the upper row in Fig. 5.

Type II. For a large a and Q , the two regions get deformation like orange segments and separated from each other. With a increasing γ , the two separated regions will grow until touching each other and take a deformation. If we keep

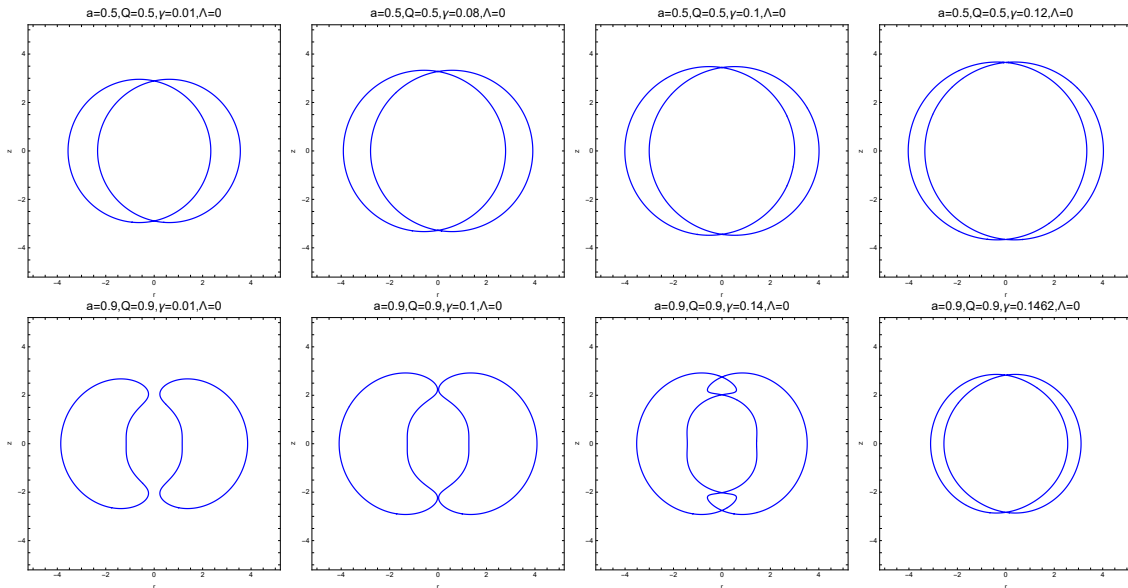


Figure 5: Shape of photon regions with fixed a and Q for a set of values of parameters γ

pushing up the value of γ , the two regions will go back to crescent shape and shrink, as shown in the lower row of Fig. 5.

V. SHADOW

A general method for computing shadows of black hole is that locate observers at a place near infinitely away from the black hole. And the shadow can be determined from the viewpoint of the observer. For a asymptotically flat spacetime, this method can be effective, but considering a non-zero cosmological constant, the position of the observer should be fixed. So for nonasymptotically flat spacetime, there is a difficulty that the method that locate the source and observer at infinity is no longer feasible. So in this paper, by following [18, 30] we use a different method to compute the shadows.

At first, we consider the observer at a fixed location (r_0, θ_0) where $\Delta_r > 0$ in the Boyer-Lindquist coordinates. And then we consider light rays sent from the location (r_0, θ_0) to the past. So we can characterized such lightlike geodesics into two different categories. For the first type, they get so close to the outer horizon that they absorbed by the gravity, so the light rays cannot come from our source. And what the observer can see is darkness in these directions. And for the other one, they avoid being absorbed and in these direction it is bright for the observer. And the boundary of the shadow can be get from borderline case.

Now, we chose an orthonormal tetrad

$$\begin{aligned}
e_0 &= \frac{\Xi}{\sqrt{\Delta_r \Sigma}} \left((r^2 + a^2) \partial_t + a \partial_\phi \right) \Big|_{(r_0, \theta_0)}, \\
e_1 &= \sqrt{\frac{\Delta_\theta}{\Sigma}} \partial_\theta \Big|_{(r_0, \theta_0)}, \\
e_2 &= - \frac{\Xi}{\sqrt{\Delta_\theta \Sigma \sin^2 \theta}} \left(a \sin^2 \theta \partial_t + \partial_\phi \right) \Big|_{(r_0, \theta_0)}, \\
e_3 &= - \sqrt{\frac{\Delta_r}{\Sigma}} \partial_r \Big|_{(r_0, \theta_0)},
\end{aligned} \tag{24}$$

where the e_0 represents the four-velocity of the observer, $e_0 \pm e_3$ are tangent to the principal null congruence and e_3 is along the direction towards the black hole's center. And the coordinates of light rays $\lambda(\tau)$ can be written in $(t(\tau), r(\tau), \theta(\tau), \phi(\tau))$, the tangent vector can be given as

$$\dot{\lambda} = \dot{t} \partial_t + \dot{r} \partial_r + \dot{\theta} \partial_\theta + \dot{\phi} \partial_\phi. \tag{25}$$

And this tangent vector at observer event can also be described as

$$\dot{\lambda} = \alpha (-e_0 + \sin \Upsilon \cos \Phi e_1 + \sin \Upsilon \sin \Phi e_2 + \cos \Upsilon e_3). \tag{26}$$

From Eq. (15)-(18) and Eq. (24), the scalar factor α can be obtain by

$$\alpha = g(\dot{\lambda}, e_0) = \Xi \frac{aL - E(r^2 + a^2)}{\sqrt{\Delta_r \Sigma}} \Big|_{(r_0, \theta_0)}. \tag{27}$$

By comparing Eq. (15)-(18) and Eq. (24), the coordinates Υ and Φ can be defined in terms of ξ and η . With the help of

$$\begin{aligned} R &= E^2(\Xi^2(r^2 + a^2 - a\xi)^2 - \Delta_r \eta), \\ \Theta &= E^2(\eta \Delta_\theta - \Xi^2(a \sin(\theta) - \xi \csc(\theta)^2)), \end{aligned} \quad (28)$$

one can obtain

$$\begin{aligned} \cos \Upsilon &= \frac{\Sigma \dot{r}}{\Xi E((r^2 + a^2) - a\xi)} \Big|_{(r_0, \theta_0)}, \\ \sin \Phi &= \frac{\sqrt{\Delta_r} \sin \theta}{\sqrt{\Delta_\theta} \sin \Upsilon} \left[\frac{a - \xi \csc^2 \theta}{a\xi - (r^2 + a^2)} \right] \Big|_{(r_0, \theta_0)}. \end{aligned} \quad (29)$$

The shadow's boundary curve is determined by the light rays that asymptotically approach a spherical lightlike geodesic. So one has

$$a\xi(r_p) = r_p^2 + a^2 - 4 \frac{r_p \Delta_r(r_p)}{\Delta'_r(r_p)}, \quad (30)$$

$$\eta(r_p) = \frac{16r_p^2 \Xi^2 \Delta_r(r_p)}{(\Delta'_r(r_p))^2}, \quad (31)$$

and r_p represents the radii coordinate of the limiting spherical lightlike geodesic. The boundary curve $(\Upsilon(r_p), \Phi(r_p))$ can therefore be given by inserting Eqs. (30) and (31) to Eq.(29).

To plot the shadows, we use a stereographic projection from the celestial sphere onto a plane with the Cartesian coordinates. And for simplicity, we set $\theta_0 = \frac{\pi}{2}$ and $r_0 = 50$ in our work.

$$x = -2 \tan\left(\frac{\Upsilon}{2}\right) \sin \Phi, \quad (32)$$

$$y = -2 \tan\left(\frac{\Upsilon}{2}\right) \cos \Phi. \quad (33)$$

We show the shape of shadows in different values of a and Q with a set of quintessence parameter γ in Fig. 6.

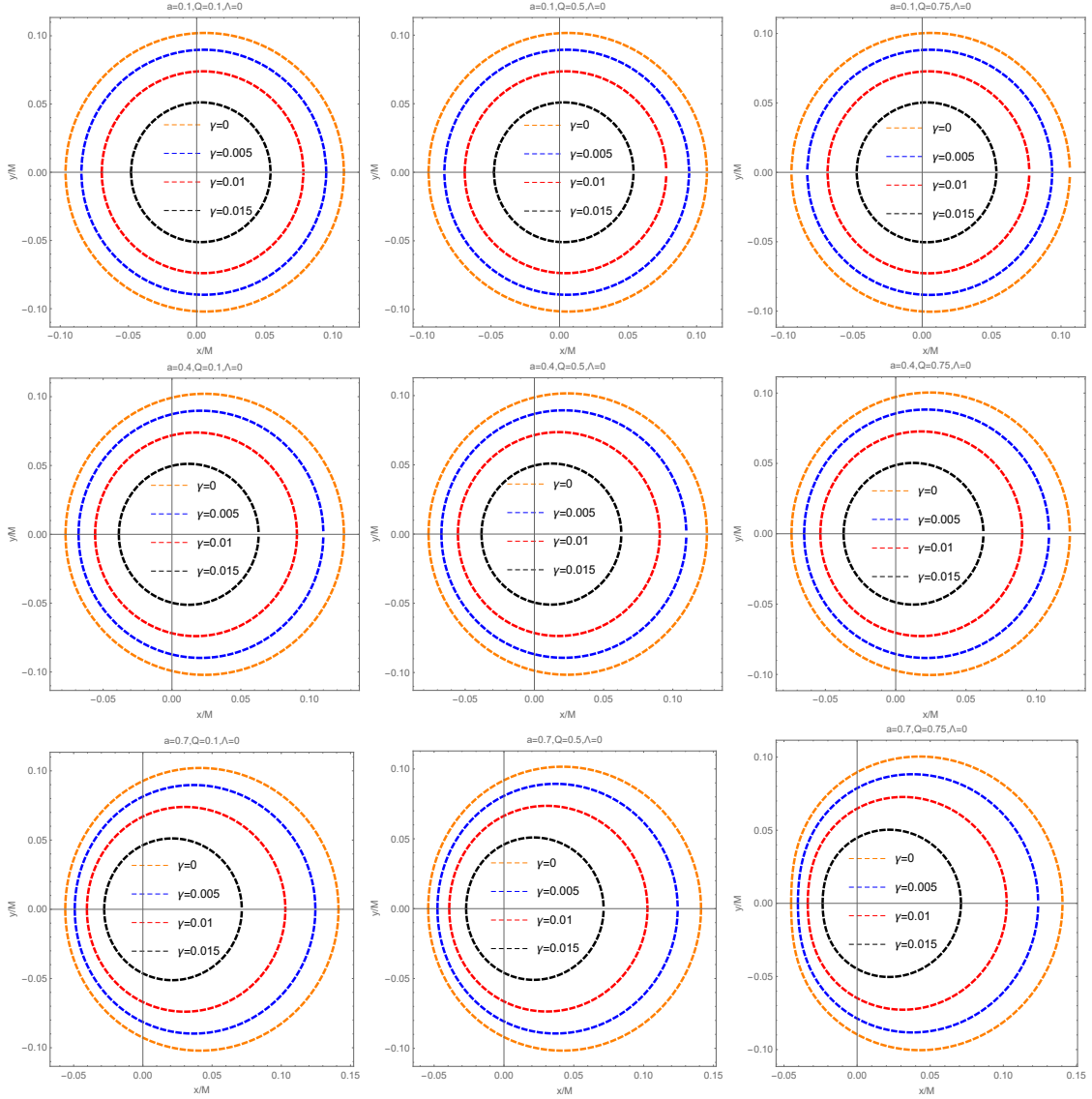


Figure 6: Shape of shadows with fixed a , Q , Λ for a set of values of parameters γ .

From Fig. 6, we can see that the spin of black hole will elongates the shadow and distorts the shadow with a increasing a . On the other hand, with a fixed a , the nonlinear magnetic charge Q will decrease the size of shadow and can also distorts the shadow. And the intensity of quintessence field will diminish the size of shadows.

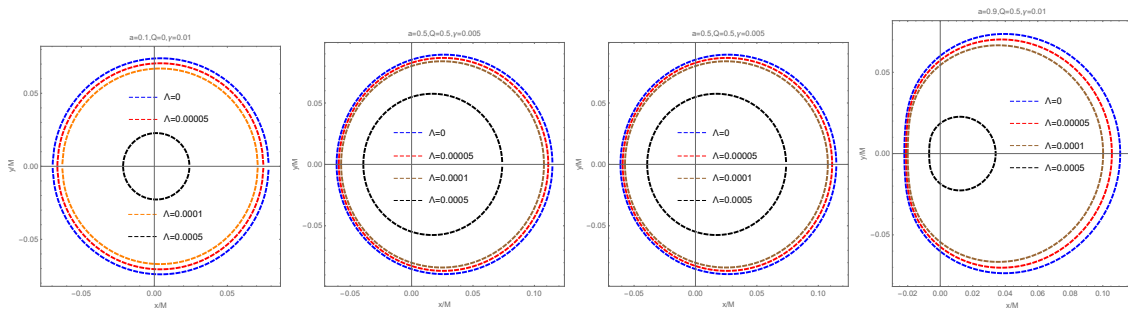


Figure 7: Shape of shadows with fixed a , Q and Λ for a set of values of parameters

Λ

Fig. 7 shows the effect of cosmological constant on the shadow for different values of a , Q and γ . From the picture, we see that the shadow maintains shapes with different values of Λ . And with an increasing value of Λ , the size of shadow decreases.

VI. CONCLUSIONS AND DISCUSSIONS

In this paper, we have obtained the solution of a nonlinear magnetic charged rotating black hole surrounded by quintessence with a cosmological constant. The structure of the black hole horizons was studied in detail. By solving the relevant equation numerically, we found that for any fixed parameters Q , γ and Λ , when $a < a_E$, the radii of inner horizons increase with the increasing a while the radii of outer horizons decrease with a . At the same time, r_Λ increase as a increase but not so obviously. For $a = a_E$, we have an extremal black hole with degenerate horizons. If $a > a_E$, no black hole will form. Similarly, for any given values of parameters a , γ and Λ , inner and outer horizons get closer first with the increase of Q , then coincide when $Q = Q_E$ and eventually disappear when $Q > Q_E$. And r_Λ increase with increasing Q but not so significantly. Furthermore, with fixed a and Q , the

cosmological horizon r_Λ significantly decrease while r_+ increase as γ or Λ increase.

And we have discussed the behavior of photon region of in details. Through graphs, we have shown the behavior of size and shape of the photon region of our black hole by varying a , Q , γ and Λ . And we find that the variation of photon region under γ can be characterized into two categories.

At last, we showed different shapes of shadow that is found by varying the intensity of quintessence, mass, magnetic charge and cosmological constant. And find the intensity of quintessence field and cosmological constant will diminish the size of shadows.

The existence of quintessence around black holes and cosmological constant play important roles in many astrophysical phenomena, so our work may provide a tool for observation of quintessence.

CONFLICTS OF INTEREST

The authors declare that there are no conflicts of interest regarding the publication of this paper.

ACKNOWLEDGMENTS

We would like to thank the National Natural Science Foundation of China (Grant No.11571342) for supporting us on this work. This work makes use of the Black Hole Perturbation Toolkit.

REFERENCES

- [1] Sheperd S Doeleman, Jonathan Weintraub, Alan EE Rogers, Richard Plambeck, Robert Freund, Remo PJ Tilanus, Per Friberg, Lucy M Ziurys, James M Moran, Brian Corey, et al. Event-horizon-scale structure in the supermassive black hole candidate at the galactic centre. *Nature*, 455(7209):78–80, 2008.
- [2] JL Synge. The escape of photons from gravitationally intense stars. *Monthly Notices of the Royal Astronomical Society*, 131(3):463–466, 1966.
- [3] J-P Luminet. Image of a spherical black hole with thin accretion disk. *Astronomy and Astrophysics*, 75:228–235, 1979.
- [4] J.M.Bardeen. in black holes (les astres occlus). *Gordon Breach Sci. Publ., New York*, page 215, 1973.
- [5] A De Vries. The apparent shape of a rotating charged black hole, closed photon orbits and the bifurcation set a_4 . *Classical and Quantum Gravity*, 17(1):123, 2000.
- [6] Kenta Hioki and Kei-ichi Maeda. Measurement of the kerr spin parameter by observation of a compact objects shadow. *Physical Review D*, 80(2):024042, 2009.
- [7] Akifumi Yumoto, Daisuke Nitta, Takeshi Chiba, and Naoshi Sugiyama. Shadows of multi-black holes: analytic exploration. *Physical Review D*, 86(10):103001, 2012.
- [8] Ahmadjon Abdujabbarov, Farruh Atamurotov, Yusuf Kucukakca, Bobomurat Ahmedov, and Ugur Camci. Shadow of kerr-taub-nut black hole. *Astrophysics and Space Science*, 344(2):429–435, 2013.
- [9] Cosimo Bambi and Katherine Freese. Apparent shape of super-spinning black holes. *Physical Review D*, 79(4):043002, 2009.

- [10] Tim Johannsen, Avery E Broderick, Philipp M Plewa, Sotiris Chatzopoulos, Sheperd S Doeleman, Frank Eisenhauer, Vincent L Fish, Reinhard Genzel, Ortwin Gerhard, and Michael D Johnson. Testing general relativity with the shadow size of sgr a. *Physical review letters*, 116(3):031101, 2016.
- [11] AE Broderick, T Johannsen, A Loeb, and D Psaltis. Testing the no-hair theorem with event horizon telescope observations of sagittarius a*, <https://doi.org/10.1088/0004-637x/784/1/7> *astrophys. J*, 784(7):1311–5564, 2014.
- [12] Adam G Riess, Alexei V Filippenko, Peter Challis, Alejandro Clocchiatti, Alan Diercks, Peter M Garnavich, Ron L Gilliland, Craig J Hogan, Saurabh Jha, Robert P Kirshner, et al. Observational evidence from supernovae for an accelerating universe and a cosmological constant. *The Astronomical Journal*, 116(3):1009, 1998.
- [13] Gary W Gibbons, Hong Lü, Don N Page, and CN Pope. Rotating black holes in higher dimensions with a cosmological constant. *Physical review letters*, 93(17):171102, 2004.
- [14] Athanasios Bakopoulos, Georgios Antoniou, and Panagiota Kanti. Novel black-hole solutions in einstein-scalar-gauss-bonnet theories with a cosmological constant. *Physical Review D*, 99(6):064003, 2019.
- [15] Shao-Wen Wei and Yu-Xiao Liu. Extended thermodynamics and microstructures of four-dimensional charged gauss-bonnet black hole in ads space. *Physical Review D*, 101(10):104018, 2020.
- [16] Volker Perlick, Oleg Yu Tsupko, and Gennady S Bisnovatyi-Kogan. Black hole shadow in an expanding universe with a cosmological constant. *Physical Review D*, 97(10):104062, 2018.
- [17] Javad T Firouzjaee and Alireza Allahyari. Black hole shadow with a cosmological constant for cosmological observers. *The European Physical Journal C*, 79(11):930, 2019.

- [18] Arne Grenzebach, Volker Perlick, and Claus Lämmerzahl. Photon regions and shadows of kerr-newman-nut black holes with a cosmological constant. *arXiv preprint arXiv:1403.5234*, 2014.
- [19] Peter AR Ade, N Aghanim, M Arnaud, Mark Ashdown, J Aumont, C Baccigalupi, AJ Banday, RB Barreiro, JG Bartlett, N Bartolo, et al. Planck 2015 results-xiii. cosmological parameters. *Astronomy & Astrophysics*, 594:A13, 2016.
- [20] VV Kiselev. Quintessence and black holes. *Classical and Quantum Gravity*, 20(6):1187, 2003.
- [21] Bobir Toshmatov, Zdeněk Stuchlík, and Bobomurat Ahmedov. Rotating black hole solutions with quintessential energy. *The European Physical Journal Plus*, 132(2):1–21, 2017.
- [22] Mahamat Saleh, Bouetou Bouetou Thomas, and Timoleon Crepin Kofane. Thermodynamics and phase transition from regular bardeen black hole surrounded by quintessence. *International Journal of Theoretical Physics*, 57(9):2640–2647, 2018.
- [23] Carlos A Benavides-Gallego, Ahmadjon Abdujabbarov, and Cosimo Bambi. Rotating and nonlinear magnetic-charged black hole surrounded by quintessence. *Physical Review D*, 101(4):044038, 2020.
- [24] Sushant G Ghosh, Sunil D Maharaj, Dharmanand Baboolal, and Tae-Hun Lee. Lovelock black holes surrounded by quintessence. *The European Physical Journal C*, 78(2):1–8, 2018.
- [25] Yu Zhang and YX Gui. Quasinormal modes of gravitational perturbation around a schwarzschild black hole surrounded by quintessence. *Classical and Quantum Gravity*, 23(22):6141, 2006.
- [26] Sushant G Ghosh. Rotating black hole and quintessence. *The European Physical Journal C*, 76(4):222, 2016.

- [27] Songbai Chen, Bin Wang, and Rukeng Su. Hawking radiation in a d-dimensional static spherically symmetric black hole surrounded by quintessence. *Physical Review D*, 77(12):124011, 2008.
- [28] Ahmadjon Abdujabbarov, Bobir Toshmatov, Zdeněk Stuchlík, and Bobomurat Ahmedov. Shadow of the rotating black hole with quintessential energy in the presence of plasma. *International Journal of Modern Physics D*, 26(06):1750051, 2017.
- [29] Mustapha Azreg-Aïnou and Manuel E Rodrigues. Thermodynamical, geometrical and poincaré methods for charged black holes in presence of quintessence. *Journal of High Energy Physics*, 2013(9):146, 2013.
- [30] Sumarna Haroon, Mubasher Jamil, Kimet Jusufi, Kai Lin, and Robert B Mann. Shadow and deflection angle of rotating black holes in perfect fluid dark matter with a cosmological constant. *Physical Review D*, 99(4):044015, 2019.
- [31] Shinji Tsujikawa. Quintessence: a review. *Classical and Quantum Gravity*, 30(21):214003, 2013.
- [32] He-Xu Zhang, Cong Li, Peng-Zhang He, Qi-Qi Fan, and Jian-Bo Deng. Optical properties of a brane-world black hole as photons couple to the weyl tensor. *European Physical Journal C*, 80(5):1–11, 2020.
- [33] H Ghaffarnejad, E Yaraie, and M Farsam. Quintessence reissner nordström anti de sitter black holes and joule thomson effect. *International Journal of Theoretical Physics*, 57(6):1671–1682, 2018.
- [34] Muhammad FAR Sakti, Agus Suroso, and Freddy P Zen. Kerr/cft correspondence on kerr-newman-nut-quintessence black hole. *The European Physical Journal Plus*, 134(11):580, 2019.
- [35] Sushant G Ghosh, Muhammed Amir, and Sunil D Maharaj. Quintessence background for 5d einstein–gauss–bonnet black holes. *The European Physical Journal C*, 77(8):530, 2017.

- [36] Meng-Sen Ma, Ren Zhao, and Ya-Qin Ma. Thermodynamic stability of black holes surrounded by quintessence. *General Relativity and Gravitation*, 49(6):79, 2017.
- [37] He-Xu Zhang, Yuan Chen, Peng-Zhang He, Qi-Qi Fan, and Jian-Bo Deng. Bardeen black hole surrounded by perfect fluid dark matter. *arXiv preprint arXiv:2007.09408*, 2020.
- [38] Wei Hong, Benrong Mu, and Jun Tao. Thermodynamics and weak cosmic censorship conjecture in the charged rn-ads black hole surrounded by quintessence under the scalar field. *Nuclear Physics B*, 949:114826, 2019.
- [39] Zhaoyi Xu and Jiancheng Wang. Kerr-newman-ads black hole in quintessential dark energy. *Physical Review D*, 95(6):064015, 2017.
- [40] M Chabab, H El Moumni, S Iraoui, K Masmarr, and S Zhizeh. More insight into microscopic properties of rn-ads black hole surrounded by quintessence via an alternative extended phase space. *International Journal of Geometric Methods in Modern Physics*, 15(10):1850171, 2018.
- [41] Mustapha Azreg-Aïnou. Charged de sitter-like black holes: quintessence-dependent enthalpy and new extreme solutions. *The European Physical Journal C*, 75(1):34, 2015.
- [42] Songbai Chen, Qiyuan Pan, and Jiliang Jing. Holographic superconductors in quintessence ads black hole spacetime. *Classical and Quantum Gravity*, 30(14):145001, 2013.
- [43] Cao H Nam. On non-linear magnetic-charged black hole surrounded by quintessence. *General Relativity and Gravitation*, 50(6):57, 2018.